Refraction contrast imaging and edge effects in neutron radiography

Article in Journal of Instrumentation · February 2012
DOI: 10.1088/1748-0221/7/02/C02047


Anton S. Tremsin
University of California, Berkeley


Eberhard Lehmann
Paul Scherrer Institut


Nikolay Kardjilov
Helmholtz-Zentrum Berlin


Markus Strobl
Paul Scherrer Institut

Refraction contrast imaging and edge effects in neutron radiography

2012 JINST 7 C02047

PUBLISHED BY IOP PUBLISHING FOR SISSA

RECEIVED: *October 2, 2011*
ACCEPTED: *January 30, 2012*
PUBLISHED: *February 22, 2012*

13th INTERNATIONAL WORKSHOP ON RADIATION IMAGING DETECTORS,
3–7 JULY 2011,
ETH ZURICH, SWITZERLAND

Refraction contrast imaging and edge effects in neutron radiography

A.S. Tremsin,[a,1] E.H. Lehmann,[b] N. Kardjilov,[c] M. Strobl,[c] I. Manke,[c] J.B. McPhate,[a] J.V. Vallerga,[a] O.H.W. Siegmund[a] and W.B. Feller[d]

[a] *Space Sciences Laboratory, University of California at Berkeley, Berkeley, CA 94720, U.S.A.*
[b] *Paul Scherer Institute, Spallation Neutron Source Division, CH-5232 Villigen, Switzerland*
[c] *Helmholtz-Zentrum Berlin, 14109 Berlin, Germany*
[d] *NOVA Scientific, Inc., 10 Picker Rd., Sturbridge, MA 01566, U.S.A.*

E-mail: ast@ssl.berkeley.edu

ABSTRACT: This paper reports on the edge enhancement and refraction/scattering effects in neutron radiography measured at thermal and cold neutron beams with a high resolution (~55 μm) microchannel plate neutron counting detector. These effects in some cases can enhance the contrast of certain features in the neutron radiographic images. At the same time, the edge effects introduce image distortions, as in case of tomographic reconstructions. The edge effects in radiographies of several steel and aluminum objects are shown for different beam divergences and sample orientations relative to the beam. It is also demonstrated how novel microcapillary neutron collimators can enable refraction and scattering contrast imaging in some cases, where the refraction and scattering angles are relatively large. These collimators can also be used to reduce some refraction artifacts, namely remove bright edges in the transmission images.

KEYWORDS: Instrumentation for neutron sources; Inspection with neutrons; Neutron radiography; Neutron sources

[1] Corresponding author.

doi:10.1088/1748-0221/7/02/C02047

2012 JINST 7 C02047

Contents

2012 JINST 7 C02047

1 Introduction

Following the advances in X-ray imaging several new imaging modalities have been demonstrated recently in thermal and cold neutron radiography [1]–[4]. While conventional radiography and tomography are based on neutron attenuation contrast (due to both absorption and scattering) the relatively novel imaging techniques exploiting propagation and grating-based diffraction contrast as well as phase contrast have been demonstrated with neutrons [5]–[10]. These imaging modalities enable unique non-destructive testing techniques that are complimentary to the measurements performed with X-rays. Existence of absorption, refraction and scattering contrasts in neutron radiographic images has been observed with certain materials and geometries, e.g. aluminium and steel objects with flat and curved surfaces illuminated at grazing incidence. In certain cases, where the variation of the neutron attenuation coefficient across the sample is very low the existence of these effects substantially enhances the image contrast [11]. However, in some cases these effects introduce unwanted distortions and should not be confused with real features of objects under study.

This paper does not present a thorough study of refraction/scattering/reflection effects in neutron radiography, but rather demonstrates several practical examples of where these effects are present and should be taken into account, as well as demonstrates how some of the image distortion can be eliminated by our neutron collimators. We also describe our first attempt to use compact collimators for refraction contrast imaging. A thorough and systematic study of edge effects differentiating between refraction, scattering and reflection needs to be conducted for their full quantitative description enabling accurate interpretation of experimental data.

One of the typical examples of image distortions is shown in figure 1, where a bright halo is seen around a steel nozzle. The high contrast of the steel imaged in a cold neutron beam does not benefit from the edge enhancement in that case and only introduces a bright feature not present in the real sample.

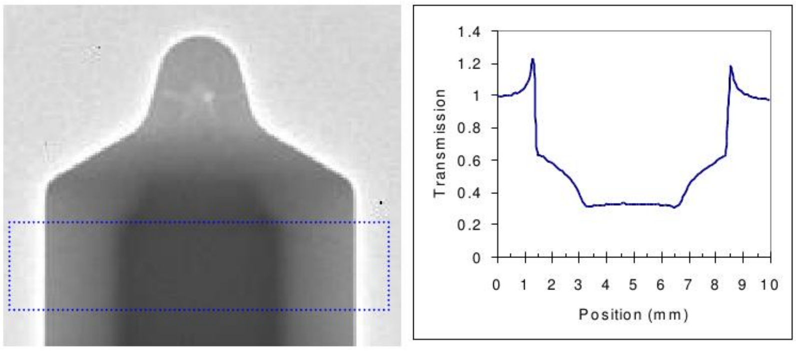

Figure 1. (Left) Radiography of a stainless steel injection nozzle performed at ICON beamline. (Right) Cross section through the image area shown by the dotted line. The edges of the nozzle appear to be brighter by 20% than the intensity of the incoming beam. This halo around the sample introduces image distortion in tomography reconstructions.

2 Experimental setup

The experiments reported in this paper were performed at a cold neutron beamline facilities ICON [12] (Spallation Neutron Source, Paul Scherer Institute, Switzerland) and CONRAD [13] (Helmholtz Centre Berlin). In most cases the edge effects require a neutron beam with high degree of collimation and a high resolution detector. The 175:1 to 700:1 beam collimation in our experiments was determined by an input aperture installed upstream in the beam from the detector. The images were recorded by a neutron counting detector consisting of neutron sensitive microchannel plates and a Timepix readout [14] providing $\sim$55 μm spatial resolution and >50% detection efficiency [15] with no readout noise. The Pixelman data acquisition software was used during experiments [16]. The active area of this detector was limited by the size of the Timepix readout of $14\times14\,\mathrm{mm}^2$. The objects exhibiting edge enhancement in neutron radiography were placed $\sim$2 cm away from the detector active area. In some cases a set of images was taken at different tilt of object relative to the beam demonstrating the angular dependence of the edge effects.

3 Results and discussion

3.1 Edge effects in radiography of Al objects

The low attenuation coefficient of Aluminium is very useful for some experiments, where Al components are used as an invisible support structure. However, in some cases, where the thin Al parts need to be visualized it is the edge enhancement which helps to improve the image contrast and thus decrease the integration time. Typically the edges of Al objects with flat surfaces illuminated at grazing incidence consist of a bright and a dark line, figure 2. A bright line is seen at both horizontal and vertical edges, where the intensity of registered neutron flux is higher than the intensity of area around it. Those extra neutrons come from a dark line seen adjacent to the bright one. The results shown in figure 2 indicate that the intensity of the bright and dark edges is proportional to the length of flat Al surface in the direction parallel to the neutron beam and the angle of neutron illumination. The same sample tilted by few degrees relative to detector normal exhibited reduced

2012 JINST 7 C02047

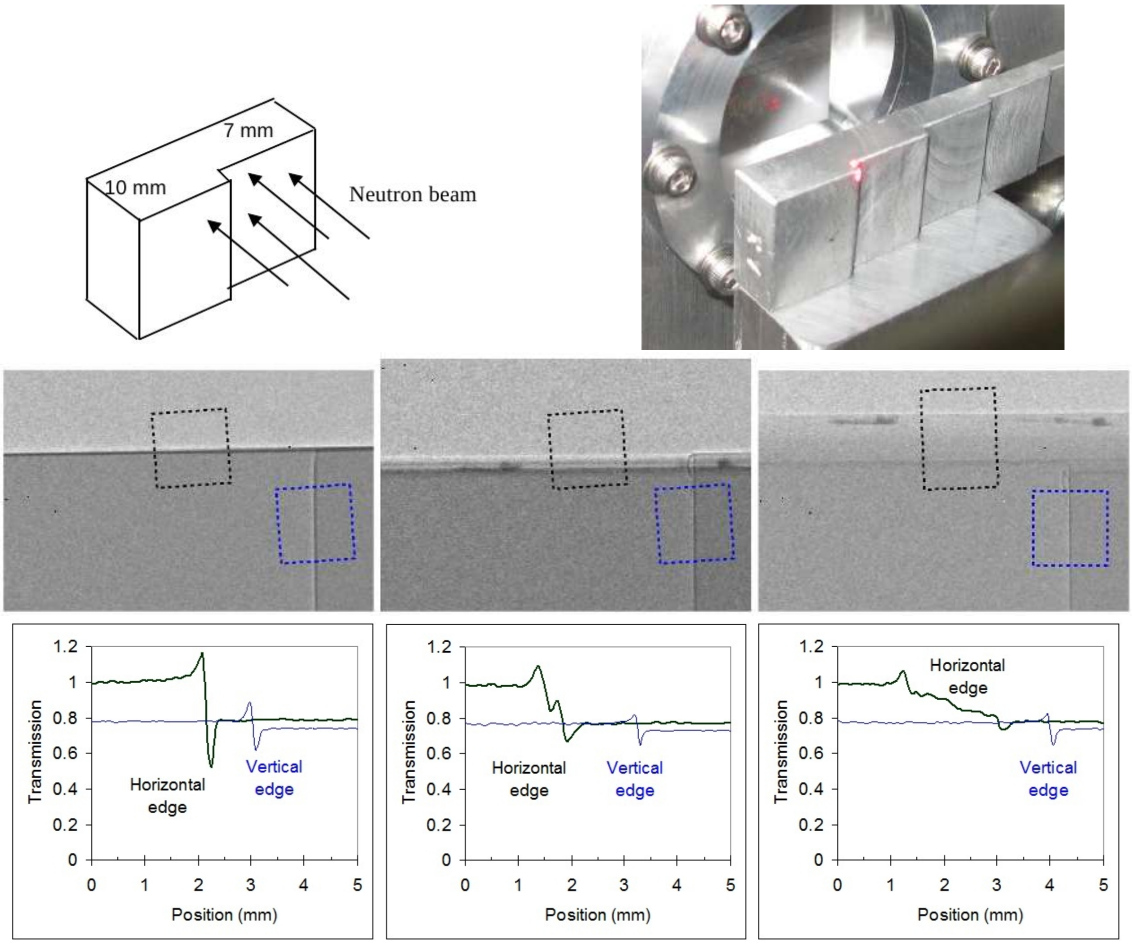

Figure 2. Edge enhancement in step-edge Al sample. ICON beamline. The edge enhancement effects are seen as narrow white and dark lines next to the edges of the sample, both in horizontal and vertical direction. Tilting the sample decreases the intensity of the bright/dark lines and moves them apart, but the width of these lines does not change substantially, indicating it is not caused by reflection off a flat surface of the sample.

edge intensity. The width and separation of the bright and dark horizontal lines increased with the tilt, while intensity of vertical lines remained nearly the same. A larger tilt (∼30 degree) substantially decreased the intensity of the edges. These results indicate that the existence of these bright and dark lines in the image is likely caused by the refraction at the edges, not by the reflection off the flat surfaces [11]. If it was due to reflection the width of the bright/dark lines should have been very wide for the large tilt of the sample.

The other Al sample with typical edge enhancement is shown in figure 3. An Al cylinder with 3 holes exhibited strong edge effects around the holes. What is interesting with this example is the fact that the edge of the same hole was bright in the case when neutrons illuminated the edge with no material behind it. At the same time the edge appeared to be dark in the image when there was Al material behind the edge. The sharpness of these edges also indicates that they are likely caused by the refraction rather than by reflection off the Al surfaces.

2012 JINST 7 C02047

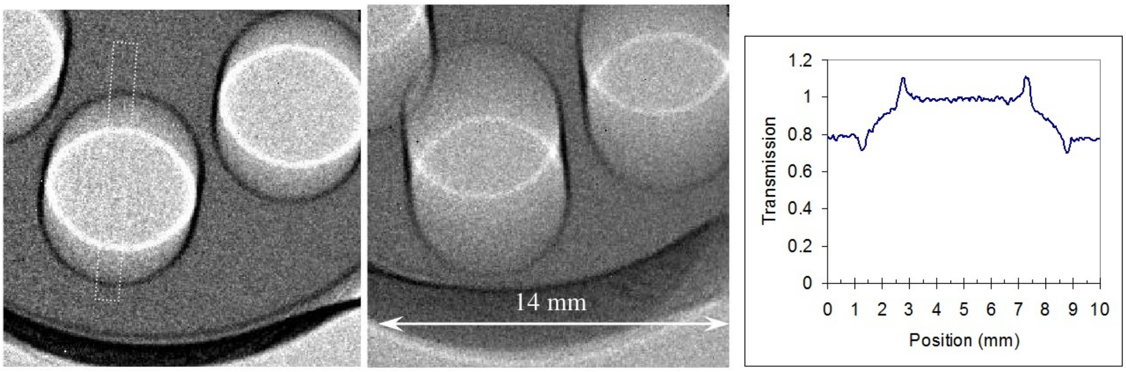

Figure 3. Radiography of an Al cylinder with three holes obtained at two different tilt angles relative to the neutron beam. Cross section through the area of the image shown by dotted line is shown on the right. ICON beamline.

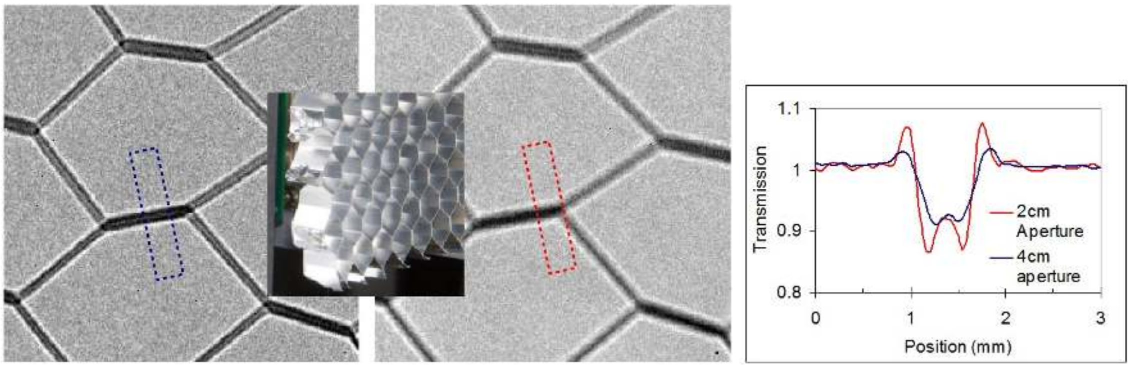

Figure 4. Neutron radiography of Al honeycomb support structure (photo insert in the middle, built from ∼10 mm wide and 50 μm thick Al foil). ICON beamline. (Left) Beam divergence of L/D=350:1. (Middle) Beam divergence of L/D=175:1. (Right) The cross sections through the images show the reduction of the edge effect for neutron beams with higher divergence.

3.2 Edge effects versus beam divergence

The intensity of the edge effects in our measurements had a strong dependence on the degree of beam collimation. A larger beam divergence substantially decreases the amplitude of the bright/dark lines, figure 4. The edges become very pronounced when both collimated beam and high resolution detector are used in radiographic experiments.

The variation of beam divergence can in fact be used to improve the contrast in some radiographic experiments enabling reduction of image integration time. An example of the possible contrast enhancement is shown in the figure 5. The same mask consisting of objects made from different materials is imaged twice: once with a beam aspect ratio of L/D=350:1 and then with L/D=175:1. Division of those two images enhances edges of some objects, which have relatively strong refraction, e.g. stainless steel needle, screws and nut, while Mg and Cu (triangular pieces) did not exhibited edge enhancement.

2012 JINST 7 C02047

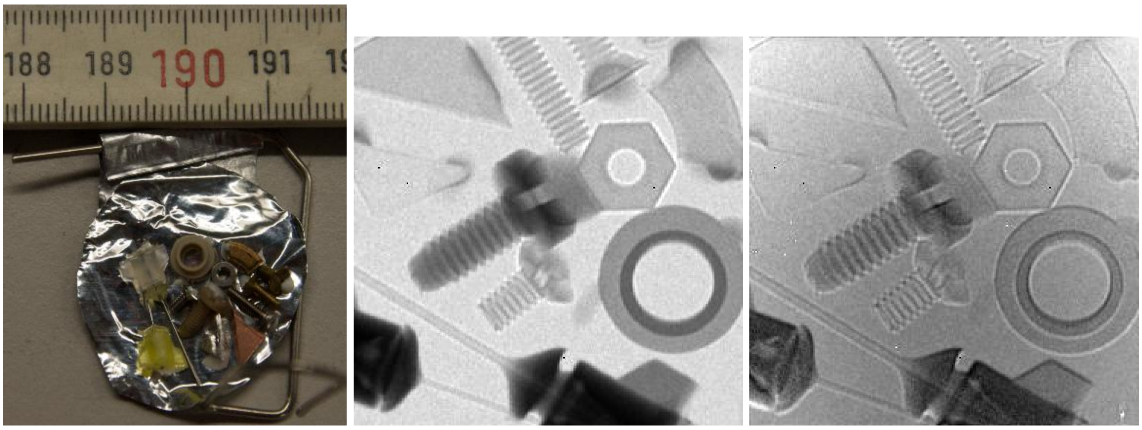

Figure 5. (Left) Imaging mask containing M2 steel and plastic screws, various pieces of copper, Mg and plastic. The objects are glued to an aluminium foil. (Middle) Neutron transmission images taken at beam divergence of 350:1. Beryllium filter is used. (Right) Division of middle image by the image taken at L/D=175:1.The division of two images emphasizes the changes due to refraction, which is weakened for the beam with a higher divergence. No changes at the edges are seen for the objects with low refraction. ICON beamline.

3.3 Reduction of edge effects by neutron collimators

The compactness of novel neutron collimators with micropores of small diameter (6–10 μm) [17]–[19] enables their placement between the object and the detector without degradation of image quality due to the beam divergence, figure 6. It was already reported how these collimators can be used to improve quantification in experiments with scattering materials by removing the scattering component from the radiographic images [19]. The small pore size of these devices results in no observable distortions of the images unless the detection resolution is better than 10 μm. However, the use of these collimators decreases the measured neutron flux at the detector as the transmission of current micropore collimators is on the scale of 55% for L/D ratios below 250:1 and only 25% for L/D$\sim$1000:1. In some experiments where the edge effects can be reduced or enhanced by these collimators the reduction in flux is compensated by the improved image quality with increased contrast.

In case these collimators are to be used to decrease the image distortions due to the edge effects they are to be aligned with the incoming neutron beam so that only neutrons parallel to the initial beam direction reach the detector, while scattered or refracted neutrons will be absorbed by the collimator. Depending on L/D ratio of collimator the range of acceptance angles can be changed. Thus the bright edges at the radiographic images can be suppressed by the collimators, while the dark edges still remain as strong as those neutrons missing in the dark edges cannot be put back by the optics. A typical example of how the bright edges are removed by a collimator with $\sim$1000:1 L/D is shown in figure 7.

3.4 Refraction contrast imaging with neutron collimators

The relatively narrow acceptance angle of neutron collimator with L/D ratio of 1000:1 of $\pm$0.2 degree can be used to enhance the contrast in imaging of objects where the attenuation contrast is

2012 JINST 7 C02047

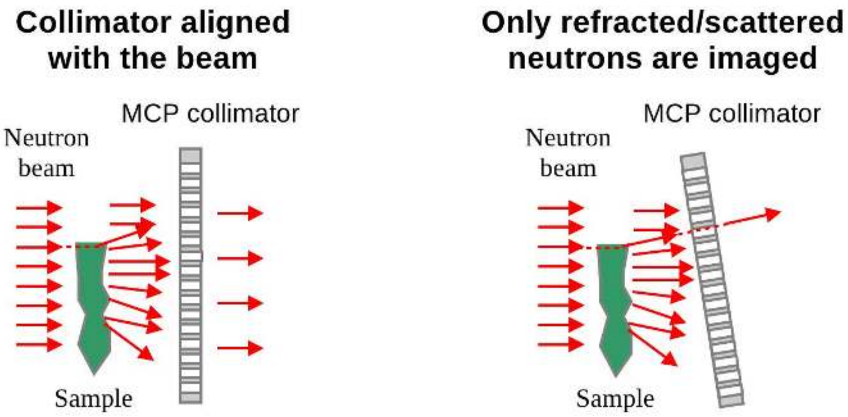

Figure 6. Schematic diagram of experiments with micropore collimators used to suppress/enhance edge effects.

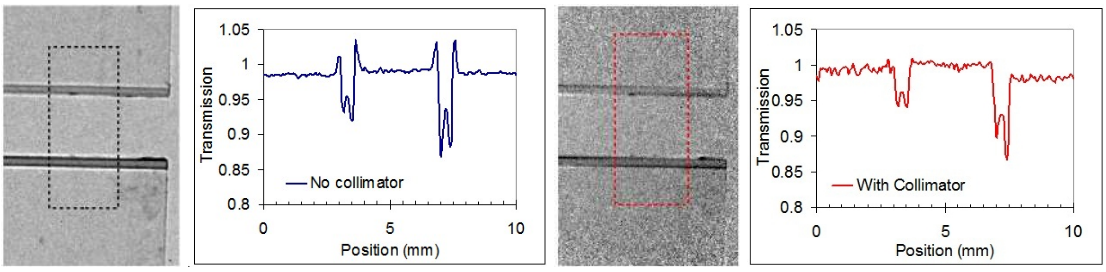

Figure 7. Elimination of bright edges by a micropore collimator with L/D ratio of ∼1000:1. (Left) An Al container walls exhibit strong edge enhancement effects in radiography experiments with well collimated cold neutron beam (L/D∼350:1). (Right) The same object imaged with collimator installed between the object and the detector. The bright edges ("extra" neutrons refracted by the edges) can be removed from the image by the collimators. No neutrons can be added where they are missing (the dark refracted edges). ICON beamline.

relatively low. In the example shown in this section the attenuation contrast was not low and we chose these objects for imaging due to their known high refraction as an easy case for the proof-of-principle experiment. A "Swagelok" fitting filled with steel beads of 1 mm diameter and small screws was imaged first with collimator aligned parallel to the incoming neutron beam, figure 8, and then imaged with collimator tilted by 0.3 degree off peak transmission in vertical direction. Tomographic reconstruction of the same object is shown in figure 9, which was performed in normal mode with no collimator installed in the beam. The ratio of radiographic images taken with collimator at 0 and 0.3 degree is shown in figure 10, where the contrast due to absorption contrast is removed and only variation of intensity due to the neutron angle deflection in the object is shown. The "Swagelock" contours almost disappeared from the image except for the lines which contain horizontal components: no vertical edges of the structure are seen in that image, as expected, since collimator was tiled in the vertical direction. The steel balls appeared to be brighter in that image as they are probably refracting neutrons stronger than the threads on the fitting due to their relatively small diameter of 1 mm. It should be noted here, that tilting the collimator by 0.3 degree was not enough to eliminate the non-refracted neutron beam completely as the combination

2012 JINST 7 C02047

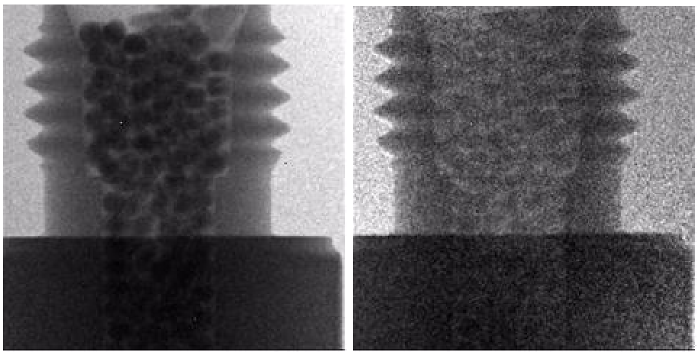

Figure 8. Neutron transmission radiography of a steel Swagelok fitting filled with 1 mm steel balls and a screw. (Left) image is taken with collimator aligned parallel to the beam transmitting mostly non-refracted neutrons. (Right) The same object imaged with collimator misaligned by 0.3 degree in vertical direction. Mostly refracted and some transmitted neutrons are imaged. The collimator with L/D ratio of 1000:1 is used in this experiment. The peak transmission of the collimator is 25%, the acceptance angular range 0.2 degree. CONRAD beamline.

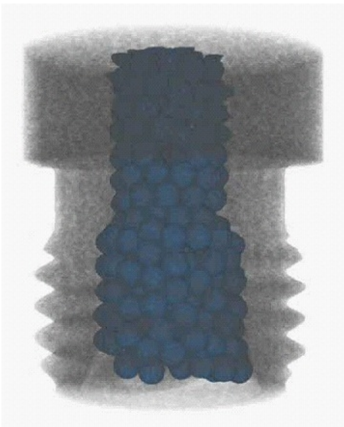

Figure 9. Tomographic reconstruction of the object radiographies of which are shown in figure 8. The 1 mm steel balls are easily seen inside the Swagelok fitting.

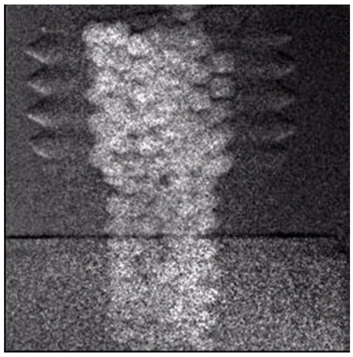

Figure 10. The refraction and small angle scattering contrast image of the object shown in figures 8,9, obtained with a neutron collimator tilted by 0.3 degree from its peak transmission, divided by the peak transmission image. The fraction of refracted and scattered neutrons in the transmitted neutron beam is enhanced by the collimator, rejecting the large fraction of transmitted neutrons. Most of the absorption features in the Swagelok fitting disappear and only the refraction in the vertical axis reveals the existence of the fitting. At the same time, the steel beads appear brighter in this image than the open beam area due to the scattering of neutrons on beads, which is enhanced in the image taken with the tilted collimator.

of limited beam divergence and the angular acceptance range of our collimator enables some non-refracted neurons to pass the filtering. It is the division of those two images which emphasized the refracted component of the image. We hope with more systematic study this method can be added to the non-conventional techniques in neutron radiography experiments, enhancing the capabilities of non-destructive investigations with thermal and cold neutrons.

2012 JINST 7 C02047

4 Conclusions

The results of our measurements with some examples of edge enhancement effects demonstrate the image distortions and, in some cases, new opportunities in thermal and cold neutron radiography. These artefacts in the images should be treated properly and not confused for the real features of more complicated objects, where it may be not easy to distinguish the edge effects from the variation of attenuation coefficient in the sample. A more detailed study of refraction/reflection and scattering at the edges is being conducted at this time. It will be very helpful for a quantitative interpretation of these phenomena in neutron radiography and shall enable an accurate interpretation of experimental data. At the same time, the application of micropore collimators can be a complimentary method in elimination of bright edges. The thin collimators with large L/D ratios can also enable improvement of image contrast by enhancing refraction features in experiments where attenuation contrast is not sufficient.

Acknowledgments

The detector used in these experiments was developed within the Medipix collaboration. The authors would like to thank AllMotion of Union City, California (www.allmotion.com) for the help with motorized stages. We greatly appreciate help of Medipix collaboration, in particular our colleagues at NiKHEF for the Muros readout electronics and data acquisition software developed by our colleagues at the Institute of Experimental and Applied Physics, Czech Technical University in Prague [16]. This work was supported in part by the U.S. Department of Energy under STTR Grants No. DE-FG02-07ER86322 and DE-FG02-08ER86353.

References

[1] M. Strobl, I. Manke, N. Kardjilov, A. Hilger, M. Dawson and J. Banhart, *Advances in neutron radiography and tomography*, *J. Phys.* **D 42** (2009) 243001.

[2] B. Schillinger, *Various neutron imaging methods at the FRM II reactor source and potential features at a spallation source installation*, *Nucl. Instrum. Meth.* **A 600** (2009) 28.

[3] E.H. Lehmann, A. Kaestner, L. Josic, S. Hartmann and D. Mannes, *Imaging with cold neutrons*, *Nucl. Instrum. Meth.* **A 651** (2011) 161.

[4] N. Kardjilov, I. Manke, A. Hilger, M. Strobl and J. Banhart, *Neutron imaging in materials science*, *Mater. Today* **14** (2011) 248.

[5] D.L. Jacobson, B.E. Allman, P.J. McMahon, K.A. Nugent, D. Paganin, M. Arif and S.A Werner, *Thermal and cold neutron phase-contrast radiography*, *Appl. Radiat. Isotopes* **61** (2004) 547.

[6] F. Pfeiffer, C. Grunzweig, O. Bunk, G. Frei, E. Lehmann and C. David, *Neutron Phase Imaging and Tomography*, *Phys. Rev. Lett.* **96** (2006) 215505.

[7] M. Strobl, W. Treimer, N. Kardjilov, A. Hilger and S. Zabler, *On neutron phase contrast imaging*, *Nucl. Instrum. Meth.* **B 266** (2008) 181.

[8] M. Strobl, C. Grünzweig, A. Hilger, I. Manke, N. Kardjilov, C. David and F. Pfeiffer, *Neutron dark-field tomography*, *Phys. Rev. Lett.* **101** (2008) 123902.

[9] M. Schulz, P. Boni, E. Calzada, M. Muhlbauer, A. Neubauer and B. Schillinger, *A polarizing neutron periscope for neutron imaging*, *Nucl. Instrum. Meth.* **A 605** (2009) 43.

[10] I. Manke et al., *Three-dimensional imaging of magnetic domains*, *Nat. Commun.* **1** (2010) 125.

[11] M. Strobl, N. Kardjilov, A. Hilger, G. Kühne and I. Manke, *High resolution investigations of edge effects in neutron imaging*, *Nucl. Instrum. Meth.* **A 604** (2009) 640.

[12] E.H. Lehmann et al., *The energy-selective option in neutron imaging*, *Nucl. Instrum. Meth.* **A 603** (2009) 429.

[13] N. Kardjilov, A. Hilger, I. Manke, M. Strobl, S. Williams, M. Dawson and J. Banhart, *Neutron tomography instrument CONRAD at HZB*, *Nucl. Instrum. Meth.* **651** (2011) 47.

[14] A.S. Tremsin et al., *High resolution neutron micro-tomography with noiseless neutron counting detector*, *Nucl. Instrum. Meth.* **A 652** (2011) 400.

[15] A.S. Tremsin, J.B. McPhate, J.V. Vallerga, O.H.W. Siegmund, W.B. Feller, E. Lehmann and M. Dawson, *Improved efficiency of high resolution thermal and cold neutron imaging*, *Nucl. Instrum. Meth.* **A 628** (2011) 415.

[16] D. Turecek, T. Holy, J. Jakubek, S. Pospisil and Z. Vykydal, *Pixelman: a multi-platform data acquisition and processing software package for Medipix2, Timepix and Medipix3 detectors*, 2011 *JINST* **6** C01046.

[17] A.S. Tremsin, W.B. Feller and R.G. Downing, *Very Compact High Performance Microchannel Plate Neutron Collimators*, *IEEE T. Nucl. Sci.* **51** (2004) 1020.

[18] A.S. Tremsin and W.B. Feller, *The theory of compact and efficient circular-pore MCP neutron collimators*,*Nucl. Instrum. Meth.* **A 556** (2005) 556.

[19] A.S. Tremsin, J.B. McPhate, E.H. Lehmann, J.V. Vallerga, O.H.W. Siegmund and W.B. Feller, *High Resolution Neutron Radiography with Very Compact and Efficient Neutron Collimators*, 2011 *JINST* **6** C01041.

2012 JINST 7 C02047